ORIGINAL RESEARCH

Turkish Journal of Immunology, 14(1):15–23

Asparagine Endopeptidase (AEP) Promotes Type I IFN Expression via the cGAS-STING Pathway by Suppressing the Activity of Apoptotic Caspases

Inam Ullah Khan[1,2], Gabriel Brooks[3], Abdus Saboor Shah[4], Yutao Zhang[5], Fang Guo[1]

[1]Ministry of Education Key Laboratory of System Biomedicine, Shanghai Jiao Tong University, Shanghai, China; [2]Department of Biochemistry, Bannu Medical College, Bannu, Khyber Pakhtunkhwa, Pakistan; [3]Department of Microbiology and Immunology, University of Maryland School of Medicine, Baltimore, MD, USA; [4]Department of Biomedical Sciences, East China Normal University School of Life Sciences, Shanghai, PR China; [5]Peking University School of Life Sciences, Beijing, China

Abstract

Objective: Fine-tuned control of interferon (IFN) induction is crucial for triggering an effective immune response that can resolve infection without causing host pathology. Apoptotic caspases (caspase-3 and caspase-9) negatively regulate virus-induced cytokine production and maintain immune homeostasis against viral infection by cleaving cyclic GMP-AMP synthase (cGAS) and interferon regulatory factor 3 (IRF3) in the cGAS-STING pathway. However, continuous unchecked suppression of interferons by these caspases would compromise innate immunity against infection. Here, we report that caspase-3 and caspase-9 themselves are regulated by asparagine endopeptidase (AEP) to maintain basal IFN levels.

Materials and Methods: We investigated the expression of IFN-β, cGAS, and IRF3, and the activity of caspase-3 and caspase-9, *in vitro* in wild-type (WT) and AEP$^{-/-}$ RAW 264.7 cells in response to vaccinia virus (VACV) infection.

Results: AEP$^{-/-}$ RAW 264.7 cells showed significantly diminished levels of IFN-β, cGAS, and IRF3, and higher caspase-3 and caspase-9 activity *in vitro* in response to VACV infection. AEP-null mice were more susceptible to VACV, and all (n=7) AEP-deficient mice succumbed to VACV on day 4, compared to WT mice, which died on day 7. This was associated with higher viral loads in the lungs (p=0.0042) and the spleen (p=0.001), and with significantly lower IFN-β levels (p=0.0018) in sera from AEP-null mice.

Conclusion: We conclude that AEP suppresses the expression and activity of caspase-3 and caspase-9 and protects cGAS and IRF3 from being completely cleaved by these apoptotic caspases. This mechanism maintains basal type I IFN production.

Keywords: Asparagine endopeptidase, apoptotic caspases, innate antiviral immunity, IFN-β

Correspondence
Fang Guo and Inam Ullah Khan

E-mail
fguo@sjtu.edu.cn and inamktk@gmail.com

Received
October 31, 2025

Accepted
December 26, 2025

Published
April 30, 2026

Suggested Citation
Khan IU, Brooks G, Shah AS, Zhang Y, Guo F. Asparagine endopeptidase (AEP) promotes type I IFN expression via the cGAS-STING pathway by suppressing the activity of apoptotic caspases. Turk J Immunol. 2026;14(1):15-23.

DOI
10.36519/tji.2026.897

Introduction

Type I interferons (IFNs) play a critical role in suppressing the spread of viral infection (1). Viral infection triggers systemic immune responses in host cells, leading to the activation of different transcriptional factors and the production of various cytokines, including type I IFNs. Released IFNs bind to interferon receptors (IFNARs) and induce the expression of numerous interferon-stimulated genes (ISGs), which interrupt almost every stage of the viral life cycle, culminating in the establishment of an antiviral state (2). However, these IFNs stimulate neighboring cells in a self-amplifying loop, thereby enhancing type I IFN production (3). Increased levels of type I IFNs have numerous immunomodulatory functions in both the innate and adaptive immune responses. Thus, increased production of type I IFNs is associated with immunopathology (4). If the immune system is too active, there is a danger of developing autoimmune disease, while a suppressed immune system may lead to infections or cancer (5). Tight control of innate immune activation is therefore crucial for inducing an effective immune response that can resolve the infection without causing host pathology.

Apoptotic caspases, particularly caspase-3 and caspase-9, contribute to the mechanisms that control innate immunity and maintain immune homeostasis against viral infection (6). Ning et al. (2) showed that apoptotic caspases suppress the production of type I IFNs by cleaving cyclic GMP-AMP synthase (cGAS) and interferon regulatory factor 3 (IRF3). Loss of caspase-3 and caspase-9 resulted in elevated type I IFN levels via the cGAS-stimulator of interferon genes (STING) pathway and enhanced innate immune responses to both DNA and RNA viruses (2).

The cGAS-STING pathway is a crucial part of the innate immune system that detects cytosolic DNA and initiates a type I IFN response to defend against infections (7). Activated by the binding of self or non-self double-stranded DNA, cGAS catalyzes the production of 2′3′-cyclic GMP-AMP (cGAMP), which in turn activates STING. Activated STING recruits and activates transcription factors like IRF3 and IRF7, which then enter the nucleus and promote the transcription of genes encoding type I IFNs and other cytokines (8). Cells from cGAS-deficient ($cGAS^{-/-}$) mice were found to be unable to produce type I IFNs and other cytokines in response to DNA transfection or DNA virus challenge (9). Asparagine endopeptidase (AEP), also known as legumain, is a lysosomal cysteine protease from the C13 peptidase family that cleaves protein substrates on the C-terminal side of asparagine (10). It plays an important role in numerous physiological and pathological processes, including immune disorders, cancer, kidney physiology, neurological diseases such as Alzheimer's disease (5,11,12), and immunity to infections (13). Asparagine endopeptidase also processes and activates a range of additional proteins (14). Mice lacking AEP were unable to generate a strong antiviral immune response against the influenza virus (13). Similarly, $AEP^{-/-}$ mice were found unable to kill *Pseudomonas aeruginosa* (13). Thus, there is increasing evidence that AEP plays a role in immunity against infections. However, its role in innate immunity to viral infection is not fully known, and its mechanism remains to be elucidated. We hypothesized that AEP is involved in innate immunity to viruses by promoting IFN-β production via the cGAS-STING pathway, thereby helping sustain the basal level of IFN secretion in cells.

Here, we report that AEP promotes the induction of type I IFN by downregulating the expression of caspase-9. Lower levels of caspase-9, in turn, suppress the activity of caspase-3, which results in increased cGAS levels, leading to basal type I IFN production that would otherwise be completely abolished.

Materials and Methods

Cells, Viral Strain, and Infection

Cell culture, viral infection, and IFN-β measurement in the culture media supernatant were performed as previously described by Khan et al. (15) Murine macrophage-like cell line RAW 264.7 and $AEP^{-/-}$ RAW 264.7 cells were cultured in 36-mm plates in Dulbecco's Modified Eagle's Medium (DMEM) supplemented with 10% fetal bovine serum (FBS) and 2 mM L-glutamine. For *in vitro* infection, cells were infected with vaccinia virus (VACV) Western Reserve (WR) strain at a multiplicity of infection (MOI) of 0.1 for 1 h after overnight incubation at 37°C. After 3 h, the culture medium was replaced with complete DMEM with 10% FBS. For the collection of endogenous proteins and mRNA, cells were grown as above and collected at 8 h post-infection. Cell supernatants were gently centrifuged at 180 g for 3 min, and an enzyme-linked immunosorbent assay (ELISA) for IFN-β was performed on the supernatants using the mouse IFN-β ELISA kit (Thermo Fisher Scientific, Waltham, MA, USA) according to the manufacturer's instructions.

Mice

AEP$^{-/-}$ mice were kindly donated by the Key Laboratory of Cell Proliferation and Differentiation, School of Life Sciences, Peking University, Beijing, China, and were maintained under specific pathogen-free conditions in an environmentally controlled facility at the School of Pharmacy, Shanghai Jiao Tong University, Shanghai, China. Mice were housed at 22°C on a 12 h/12 h light/dark cycle. Food and water were provided *ad libitum*. All experiments were conducted in accordance with the institutional ethical guidelines for animal research and were approved by the Institutional Animal Care and Use Committee (IACUC) of Shanghai Jiao Tong University, Shanghai, China.

Lentivirus-Mediated AEP Overexpression

Lentiviral vectors encoding the AEP coding sequence were constructed by Hanyin Biotechnology Co., Shanghai, China. Recombinant AEP-overexpressing lentivirus and negative control lentivirus were prepared and titrated to 10^9 transduction units (TU)/mL. For AEP overexpression, cells were grown in six-well plates at a density of 2×10^5 cells per well, followed by transfection with the pLV-EF1α-AEP-IRES-Bsd plasmid and 8 μg/mL polybrene the next day. At 72 h after viral infection, AEP expression was examined by Western blotting.

In vivo Viral Challenge

Age- and sex-matched mice were divided into three groups (wild-type [WT], AEP$^{-/-}$, and uninfected), each containing seven mice (n=7). Wild-type and AEP$^{-/-}$ groups were anesthetized with isoflurane and infected intranasally (i.n.) with VACV at $1x10^6$ plaque-forming units (PFU) per mouse in 50 μL of phosphate-buffered saline (PBS) or PBS alone. Airways were washed with 500 μL of PBS. IFN-β protein expression was quantified by quantitative real-time reverse transcription polymerase chain reaction (qRT-PCR) in total RNA extracted from lung tissue using the RNeasy mini kit (Qiagen, Hilden, Germany).

Mouse serum was collected 48 h after infection to measure IFN-β production. For gene expression, analysis or viral load in the tissue, in some experiments, mice were euthanized on day 5 after treatment to harvest the lungs. Lungs were homogenized with an Omni tissue homogenizer (Omni International, Kennesaw, GA, USA) in Opti-MEM I medium containing 25% sucrose (Life Technologies, Carlsbad, CA, USA). IFN-β levels in the lung homogenates were measured by ELISA. Viral titers were determined by standard plaque assay as previously described (16). Bone marrow-derived macrophages (BMDMs) from mice were isolated and cultured as previously described by Bailey et al. (17).

Gene Expression Analysis by Real-Time PCR

TRIzol reagent (Ambion, Austin, TX, USA) was used for RNA extraction for quantitative PCR following the manufacturer's instructions. Using 2.5 μM oligo (dT) primers and 10 U/μL SuperScript III Reverse Transcriptase (Invitrogen, Carlsbad, CA, USA), 500 ng RNA was reverse transcribed into cDNA in 20 μL final reaction volume for 5 min at 65°C. Quantitative PCR was performed on a StepOnePlus Real-Time PCR System (Applied Biosystems, Foster City, CA, USA) using 1/20 of the cDNA volume. mRNA levels of IFN-β and cGAS were measured in technical triplicate for each sample using the following primer pairs:

Mouse *Ifnb* (forward): TCCGAGCAGAGATCTTCAGGAA
Mouse *Ifnb* (reverse): TGCAACCACCACTCATTCTGAG
Mouse *Gapdh* (forward): GAAGGGCTCATGACCACAGT
Mouse *Gapdh* (reverse): GGATGCAGGGATGATGTTCT

Relative mRNA expression levels were calculated using the ΔΔCt method. Data are presented as the relative abundance of the indicated mRNA normalized to that of *Gapdh* expression.

Western Blot Analysis

For measurement of cGAS, IFN-β, caspase-3, caspase-9, and phosphorylated IRF3 (p-IRF3) by Western blotting, $1x10^6$ RAW 264.7 and AEP$^{-/-}$ RAW 264.7 cells were grown at 37°C in 36-mm plates in DMEM supplemented with 10% FBS and 2 mM L-glutamine. Cells were suspended in Laemmli sample buffer containing 5% β-mercaptoethanol (β-ME), followed by boiling for 5 min. Protein concentration was measured using a BCA Protein Assay Kit (Thermo Fisher Scientific, Waltham, MA, USA). Equal amounts of protein (50 μg) were run on 10% sodium dodecyl sulfate–polyacrylamide gel electrophoresis (SDS-PAGE), transferred onto nitrocellulose membranes, and blocked with 5% non-fat milk in Tris-buffered saline with Tween-20 (TBST) for 2 h at room temperature. Membranes were incubated overnight at 4°C with primary antibodies against GAPDH, cGAS, IFN-β, caspase-3, caspase-9, and p-IRF3, followed by incubation with the appropriate horseradish peroxidase (HRP)–conjugated secondary antibodies. Protein bands were visualized using enhanced chemiluminescence (ECL) substrate and imaged.

Assay for Caspase-3 and Caspase-9 Activities

Activities of caspase-3 and caspase-9 were measured colorimetrically using caspase-3 and caspase-9 Activity kits (Beyotime Biotechnology, Nanjing, China). A total of 1×10^6 cells were washed with cold PBS and lysed on ice, followed by centrifugation at 16,000–20,000 g for 15 min at 4°C. Caspase assays were performed in 96-well plates by incubating 50 µL supernatant per sample with 10 µL caspase substrate and 40 µL reaction buffer for 1.5 h at 37°C. Absorbance was read at 450 nm using a microplate reader (MK3, Thermo Fisher Scientific, Waltham, MA, USA).

Viral Plaque Assay

Viral plaque assay was performed as described by Khan et al. (18). Organs from control or virus-infected mice were homogenized, followed by three freeze-thaw cycles to release the virus. For VACV infectivity quantification, BS-C-1 cell monolayers were infected with virus culture medium containing 2% (wt/vol) methylcellulose. After 2 days, cells were stained with 0.1% crystal violet solution, plaques were counted, and average counts were multiplied by the dilution factor to determine the viral titer as PFU per mL.

Statistical Analysis

All data are presented as mean ± standard error of the mean (SEM) of at least three experiments. Statistical significance was determined using a two-tailed Student's t-test, with $p<0.05$ considered statistically significant. For mouse survival studies, Kaplan-Meier survival curves were generated using GraphPad Prism version 10.3 (GraphPad Software, Boston, MA, USA).

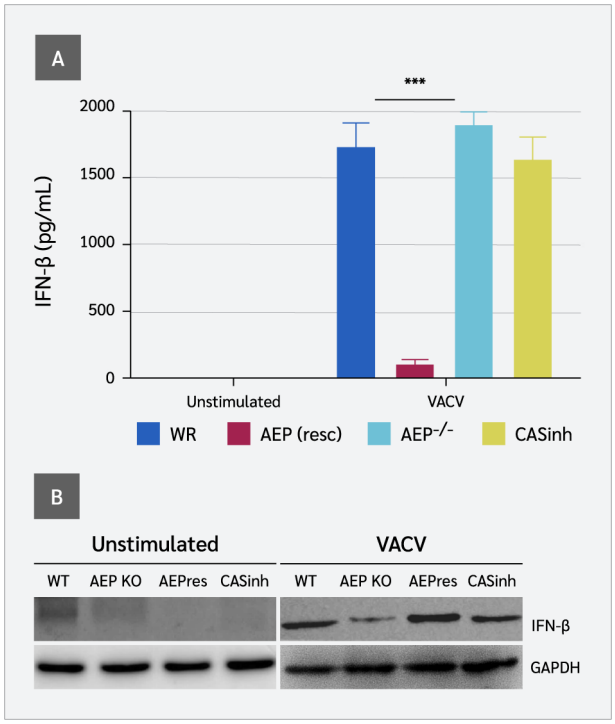

Figure 1. Effect of AEP on IFN-β expression.

Wild-type RAW 264.7, AEP$^{-/-}$, and AEP-reconstituted RAW 264.7 cells were cultured in 36-mm dishes in DMEM supplemented with 10% FBS and 2 mM L-glutamine. Following overnight incubation at 37°C, cells were infected with VACV and maintained at 37°C for 8 h. IFN-β levels in cell culture supernatants were measured by ELISA. For analysis of endogenous protein expression, cells were harvested after 8 h.

(A) IFN-β levels in cell culture supernatants. **(B)** Immunoblot analysis of IFN-β expression.

Data are presented as mean ± standard error of the mean from three independent experiments. *** represents p-value < 0.005

WT: Wild-type, **AEP:** Asparagine endopeptidase, **AEPresc:** AEP-reconstituted, **CASinh:** Caspase inhibitor–treated, **cGAS:** Cyclic GMP-AMP synthase, **AEP KO:** AEP knockout, **p-IRF3:** Phosphorylated interferon regulatory factor 3, **VACV:** Vaccinia virus, **GAPDH:** Glyceraldehyde-3-phosphate dehydrogenase.

Results

AEP$^{-/-}$ Cells Express Lower Levels of IFN-β

We first assessed the expression of IFN-β in WT and AEP$^{-/-}$ RAW 264.7 cells in response to VACV infection by measuring IFN-β in cell supernatants using an IFN-β bioassay. The ability of AEP-null cells to induce IFN-β was severely compromised. A significantly diminished level of IFN-β was detected in the supernatants from AEP-null cells in response to VACV infection ($p<0.005$) compared to WT cells (Figure 1A and 1B). Unlike cGAS-null cells, in which IFN levels were completely undetectable (19), IFN-β remained detectable at very low levels in the supernatants of AEP$^{-/-}$ RAW 264.7 cells following VACV infection. However, when AEP was rescued in AEP$^{-/-}$ cells, IFN-β levels were also restored. Interestingly, pharmacological inhibition of AEP$^{-/-}$ RAW 264.7 cells with z-VAD-fmk, a broad-spectrum inhibitor of caspases, enhanced IFN-β production following VACV infection.

AEP$^{-/-}$ Cells Express Low Levels of cGAS and p-IRF3

Because VACV induces type I IFNs via the cGAS-STING pathway, we hypothesized that the compromised production of IFN-β might result from disruption of the cGAS-STING pathway. Therefore, we examined the expression levels of key proteins in this pathway, i.e., cGAS and p-IRF3. Significantly lower levels of endogenous cGAS were detected in virally infected AEP-null cells, as shown by the

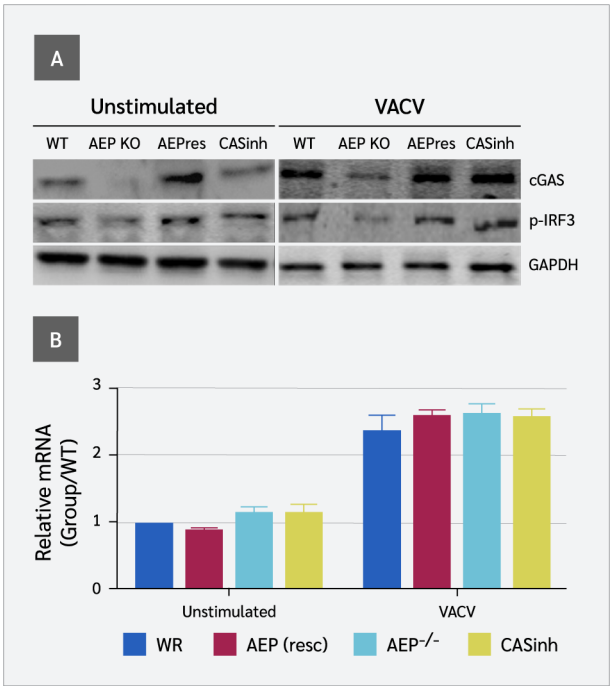

Figure 2. Effect of AEP on cGAS expression and p-IRF3 phosphorylation.

Wild-type RAW 264.7, AEP$^{-/-}$ RAW 264.7, and AEP-reconstituted RAW 264.7 cells were cultured in 36-mm dishes in DMEM supplemented with 10% FBS and 2 mM L-glutamine. Following overnight incubation at 37°C, cells were infected with VACV and maintained at 37°C for 8 h. For analysis of endogenous proteins and mRNA, cells were harvested after 8 h.

(A) Western blot analysis showing the expression of full-length cGAS and p-IRF3. **(B)** Relative cGas mRNA levels normalized to the unstimulated wild-type control, which was set to 1.

Data are presented as mean ± standard error of the mean from three independent experiments.

WT: Wild-type, **AEP:** Asparagine endopeptidase, **AEPresc:** AEP-reconstituted, **CASinh:** Caspase inhibitor–treated, **cGAS:** Cyclic GMP-AMP synthase, **AEP KO:** AEP knockout, **p-IRF3:** Phosphorylated interferon regulatory factor 3, **VACV:** Vaccinia virus, **GAPDH:** Glyceraldehyde-3-phosphate dehydrogenase.

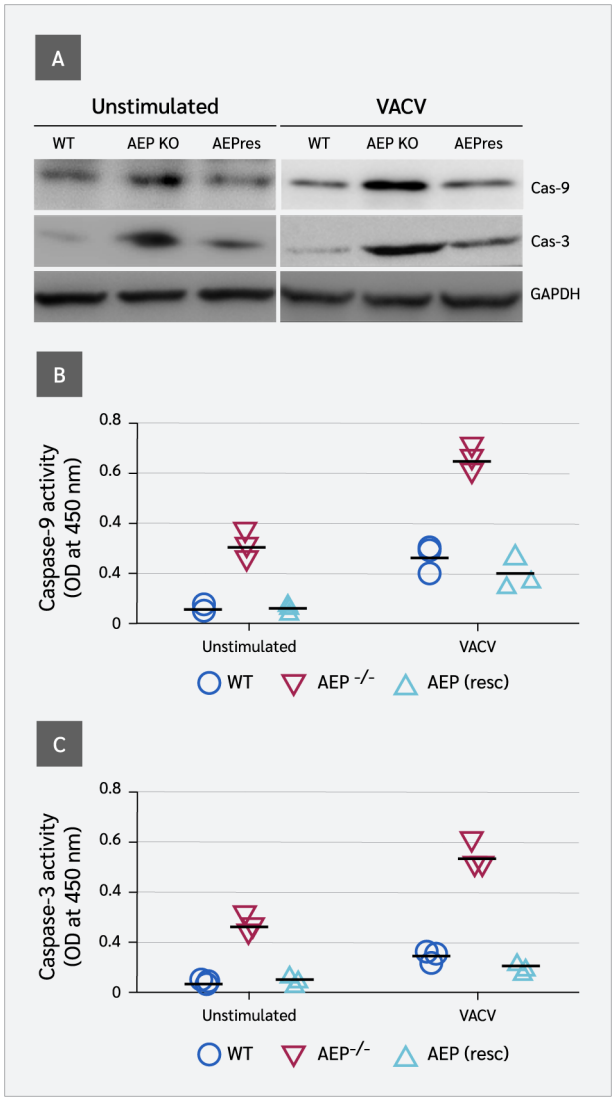

Figure 3. Effect of AEP on the expression and activity of caspase-9 and caspase-3.

Wild-type RAW 264.7, AEP$^{-/-}$ RAW 264.7, and AEP-reconstituted RAW 264.7 cells were cultured in 36-mm dishes in DMEM supplemented with 10% FBS and 2 mM L-glutamine. Following overnight incubation at 37°C, cells were infected with VACV and maintained at 37°C. For analysis of endogenous proteins, cells were harvested after 8 h.

(A) Western blot analysis showing the expression of caspase-9 and caspase-3. **(B)** Caspase-9 activity measured colorimetrically at 450 nm. (C) Caspase-3 activity measured colorimetrically at 450 nm.

Data are presented as mean ± standard error of the mean (SEM) from three independent experiments.

WT: Wild-type, **AEP:** Asparagine endopeptidase, **AEPresc:** AEP-reconstituted, **CASinh:** Caspase inhibitor–treated, **cGAS:** Cyclic GMP-AMP synthase, **AEP KO:** AEP knockout, **p-IRF3:** Phosphorylated interferon regulatory factor 3, **VACV:** Vaccinia virus, **GAPDH:** Glyceraldehyde-3-phosphate dehydrogenase.

loss of full-length cGAS protein (Figure 2A). However, qPCR results did not match well with the immunoblot results. At the mRNA level, we detected a small, non-significant decrease in cGAS expression in AEP-null cells (Figure 2B). These results imply that the reduction in cGAS did not occur at the expression level but rather at the protein level.

The decrease in cGAS was further assessed by its ability to catalyze the synthesis of cGAMP, which was assessed by measuring IRF3 dimerization (phosphorylation) using native gel electrophoresis. A significant decrease in IRF3 phosphorylation was observed in AEP-null cells in response to VACV infection, indicating reduced cGAMP production compared to WT cells. However, in AEP rescued cells, both cGAS and p-IRF3 levels were restored (Figure 2A). These results correlated with the presence or absence

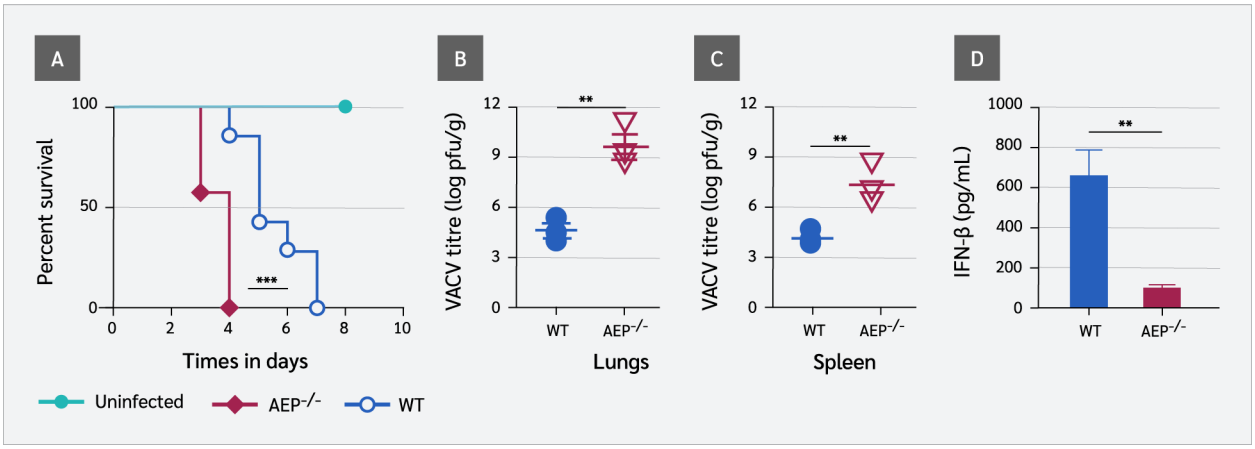

Figure 4. Characterization of the *in vivo* response to VACV infection in AEP-deficient mice.

Mice were infected by intranasal (i.n.) administration of VACV. Mice were euthanized at 5 h post infection for serum and tissue collection.
(A) Survival of WT and AEP$^{-/-}$ mice over a 10-day period (n=7) following intranasal infection with VACV (1 × 10^6 PFU/mouse). **(B)** VACV titers in the lungs and **(C)** Spleens of WT and AEP$^{-/-}$ mice (n=7). **(D)** IFN-β levels in lung tissues of WT and AEP$^{-/-}$ mice (n=7).

WT: Wild-type, **AEP:** Asparagine endopeptidase, **VACV:** Vaccinia virus.

Table 1. Summary of *in vivo* study results.

Assay/parameter	Uninfected	WT	AEP$^{-/-}$	*p*-value
Survival time (days post challenge)	10	7	4	0.0019
Lung viral titer (log PFU/g)	-	4.66	9.61	0.0042
Spleen viral titer (log PFU/g)	-	4.03	7.27	0.001
Lungs IFN-β (pg/mL)	ND	660	97	0.0018

AEP: Asparagine endopeptidase, **IFN-β:** Interferon beta, **PFU:** Plaque-forming unit, **WT:** Wild-type, **ND:** Not detected
(*) indicates *p*-value ≤ 0.05, (**) indicates *p*-value ≤ 0.01, (***) indicates P-value ≤ 0.001

of AEP and the level of IFN-β produced by WT and AEP-null cells. Together, these findings show a positive correlation between the presence of AEP and components of the cGAS-STING pathway involved in IFN-β induction.

AEP$^{-/-}$ Cells Show Enhanced Apoptotic Caspase Activity

Previous studies have shown that apoptotic caspases (caspase-9 and caspase-3) suppress type I IFN production by inactivating cGAS and IRF3 (2). We investigated the effect of AEP on the expression and activity of these caspases. AEP$^{-/-}$ cells displayed elevated levels of caspase-9 compared to WT cells (Figure 3A). Colorimetric results showed that caspase-9 activities were significantly higher in AEP-null cells than in WT cells. These results suggest that AEP suppresses the expression and activity of caspase-9. As caspase-3 acts downstream of caspase-9 and its activity is modulated by caspase-9, caspase-3 expression and activity were also significantly higher in AEP-null cells compared to WT cells. However, in AEP-reconstituted cells, the expression and activity of both caspases were repressed.

AEP Augments Host Resistance to Viral Infection

We first assessed the expression levels of cGAS, IRF3, caspase-9, and caspase-3 in BMDMs from WT and AEP-null mice. We detected significantly lower levels of cGAS and IRF3 and elevated levels of caspase-3 and caspase-9 (Figure 4E). To determine the contribution of AEP to the innate immune response against viral infection, we next evaluated *in vivo* evidence. Antiviral experiments

were performed in WT and AEP$^{-/-}$ mice. Wild-type and AEP$^{-/-}$ mice were infected with VACV (1×10^6 PFU/mouse), and lung inflammation was monitored on day 4 post-infection.

AEP-null mice are fertile and viable with no overt behavioral abnormality, although their body weights are reduced compared with WT littermates (20,21). We found that AEP-null mice were more susceptible to VACV infection, and all AEP-deficient mice (n=7) succumbed to VACV by day 4, whereas WT mice died on day 7 (Figure 4A). This was associated with higher viral loads in the lungs (p=0.0042) (Figure 4B) and the spleen (p=0.001) (Figure 4C) of AEP-null mice. This finding was consistent with the significantly lower IFN-β level (p=0.0018) in the sera of AEP-null mice (Figure 4D). A summary of the results from *in vivo* studies is presented in Table 1.

Discussion

Interferons are vital for host defense against viral infection and are constitutively expressed at low levels in cells (22). Such steady state IFN production is important for innate immune homeostasis in the absence of infection (22). However, aberrant interferon production leads to immunopathology or increased susceptibility to infections (15). Therefore, tight regulation of IFNs is critical for initiating effective immunity while avoiding inflammation. Our study revealed that AEP suppresses the expression and activity of apoptotic caspase-3 and caspase-9 and provides molecular insight into the coordination between AEP and antiviral innate immune activation.

Ning et al. (2) showed that apoptotic caspases (caspase-9 and caspase-3) negatively regulate virus-induced cytokine production by mediating cGAS and IRF3 cleavage to prevent excessive type I IFN induction and the resulting innate immune activation. However, uncontrolled or excessive cleavage of these proteins would be detrimental to the host. This necessitates a mechanism to prevent caspase-mediated excessive inactivation of cGAS and IRF3 while ensuring steady-state IFN production. Asparagine endopeptidase represents a simple but efficient way to fulfill this role. We showed that the activities of these caspases are under the control of AEP. Asparagine endopeptidase suppresses apoptotic caspase activity and thereby regulates type I IFN expression via the cGAS-STING pathway to establish an antiviral state. The results of the study by Sun et al. (23) support our findings, demonstrating that AEP suppresses caspase-3 and caspase-9 activity.

Our *in vitro* results show that in AEP-deficient RAW 264.7 cells, the expression and activity of caspase-3 and caspase-9 were significantly elevated. Based on the findings of Ning et al. (2), this increase would be expected to result in diminished levels of IFN-β, cGAS, and IRF3. Consistent with this expectation, the ability of AEP$^{-/-}$ RAW 264.7 cells to induce IFN-β was severely compromised. Similarly, the ability of these cells to express cGAS and to induce IRF3 phosphorylation was also markedly reduced. These findings were correlated with the elevated expression and activity of caspase-3 and caspase-9.

In vivo results further support our conclusion that AEP suppresses and regulates apoptotic caspase activity to establish an antiviral state. We found that AEP-null mice were more susceptible to VACV infection, and all AEP-deficient mice succumbed to infection by day 4, whereas WT mice died on day 7, which was associated with higher viral loads in the lungs and spleen of AEP-null mice. This was consistent with the significantly lower levels of cGAS and IRF3 in the BMDMs from AEP-deficient mice and reduced IFN-β levels in the sera. These findings are supported by Maschalidi et al. (13), who reported that AEP-deficient mice are unable to generate a strong antiviral response.

Our findings support the conclusion that AEP promotes type I IFN expression in mice via the cGAS-STING pathway by suppressing apoptotic caspase activity. This mechanism helps to maintain basal type I IFN production. However, the direct translation of murine experimental data to human physiology and pathological conditions is not straightforward due to important differences between mice and humans in immune defense strategies and pathogen responses. Liu et al. reported that cGAS activation mechanisms differ between mice and humans (24). Nevertheless, because the core components of this pathway—AEP, apoptotic caspases, and cGAS-STING—are highly conserved, these findings remain biologically relevant to human physiology. Further validation will require experimental confirmation.

Conclusion

We conclude that AEP suppresses the expression and activity of apoptotic caspase-3 and caspase-9, thereby

protecting cGAS and IRF3 from excessive cleavage and ensuring basal type I IFN production. These findings suggest that AEP plays an important role in maintaining finely tuned innate immune homeostasis during microbial infection.

Ethical Approval: The study was approved by the Shanghai Jiaotong University Institutional Animal Care and Use Committee (IACUC), on December 20, 2020, with the decision number A 2017054.

Informed Consent: N.A.

Peer-review: Externally peer-reviewed

Author Contributions: Concept – I.U.K., F.G.; Design – I.U.K., F.G.; Supervision – F.G.; Fundings – F.G.; Materials – I.U.K., A.S.S., Y.Z.; Data Collection and/or Processing – I.U.K., G.B., Y.Z.; Analysis and/or Interpretation – I.U.K., Y.Z., A.S.S; Literature Review – F.G., I.U.K.; Writer – I.U.K., G.B.; Critical Reviews – F.G., A.S.S., G.B.

Conflict of Interest: The authors declare no conflict of interest.

Financial Disclosure: The authors declared that this study has received no financial support.

Acknowledgment: The authors thank Shanghai Sorrento Medical Technology Co., Ltd. for technical support for this study.

References

1 Choubey D, Moudgil KD. Interferons in autoimmune and inflammatory diseases: regulation and roles. J Interferon Cytokine Res. 2011;31(12):857–65. [CrossRef]

2 Ning X, Wang Y, Jing M, Sha M, Lv M, Gao P, et al. Apoptotic caspases suppress type I interferon production via the cleavage of cGAS, MAVS, and IRF3. Mol Cell. 2019;74(1):19–31. e7. [CrossRef]

3 Baccala R, Hoebe K, Kono DH, Beutler B, Theofilopoulos AN. TLR-dependent and TLR-independent pathways of type I interferon induction in systemic autoimmunity. Nat Med. 2007;13(5):543–51. [CrossRef]

4 Marshak-Rothstein A. Toll-like receptors in systemic autoimmune disease. Nat Rev Immunol. 2006;6(11):823–35. [CrossRef]

5 Zhang Z, Xie M, Ye K. Asparagine endopeptidase is an innovative therapeutic target for neurodegenerative diseases. Expert Opin Ther Targets. 2016;20(10):1237–45. [CrossRef]

6 Chen H, Ning X, Jiang Z. Caspases control antiviral innate immunity. Cell Mol Immunol. 2017;14(9):736–47. [CrossRef]

7 Ishikawa H, Ma Z, Barber GN. STING regulates intracellular DNA-mediated, type I interferon-dependent innate immunity. Nature. 2009;461(7265):788–92. [CrossRef]

8 Sun L, Wu J, Du F, Chen X, Chen ZJ. Cyclic GMP-AMP synthase is a cytosolic DNA sensor that activates the type I interferon pathway. Science. 2013;339(6121):786–91. [CrossRef]

9 Anghelina D, Lam E, Falck-Pedersen E. Diminished innate antiviral response to adenovirus vectors in cGAS/STING-deficient mice minimally impacts adaptive immunity. J Virol. 2016;90(13):5915–27. [CrossRef]

10 Song M. The asparaginyl endopeptidase legumain: an emerging therapeutic target and potential biomarker for Alzheimer's disease. Int J Mol Sci. 2022;23(18):10223. [CrossRef]

11 Miller G, Matthews SP, Reinheckel T, Fleming S, Watts C. Asparagine endopeptidase is required for normal kidney physiology and homeostasis. FASEB J. 2011;25(5):1606–17. [CrossRef]

12 Zhao L, Hua T, Crowley C, Ru H, Ni X, Shaw N, et al. Structural analysis of asparaginyl endopeptidase reveals the activation mechanism and a reversible intermediate maturation stage. Cell Res. 2014;24(3):344–58. [CrossRef]

13 Maschalidi S, Hässler S, Blanc F, Sepulveda FE, Tohme M, Chignard M, et al. Asparagine endopeptidase controls anti-influenza virus immune responses through TLR7 activation. PLoS Pathog. 2012;8(8):e1002841. [CrossRef]

14 Freeley S, Cardone J, Günther SC, West EE, Reinheckel T, Watts C, et al. Asparaginyl endopeptidase (legumain) supports human Th1 induction via cathepsin l-mediated intracellular C3 activation. Front Immunol. 2018;9:2449. [CrossRef]

15 Khan IU, Brooks G, Guo NN, Chen J, Guo F. Fever-range hyperthermia promotes cGAS-STING pathway and synergizes DMXAA-induced antiviral immunity. Int J Hyperthermia. 2021;38(1):30–7. [CrossRef]

16 Khan IU, Ahmad F, Zhang S, Lu P, Wang J, Xie J, et al. Respiratory syncytial virus F and G protein core fragments fused to HBsAg-binding protein (SBP) induce a Th1-dominant immune response without vaccine-enhanced disease. Int Immunol. 2019;31(4):199–209. [CrossRef]

17 Bailey JD, Shaw A, McNeill E, Nicol T, Diotallevi M, Chuaiphichai S, et al. Isolation and culture of murine bone marrow-derived macrophages for nitric oxide and redox biology. Nitric Oxide. 2020;100–101:17–29. [CrossRef]

18 Khan IU, Huang J, Li X, Xie J, Zhu N. Nasal immunization with RSV F and G protein fragments conjugated to an M cell-targeting ligand induces an enhanced immune response and protection against RSV infection. Antiviral Res.

2018;159:95–103. [CrossRef]

19 Li XD, Wu J, Gao D, Wang H, Sun L, Chen ZJ. Pivotal roles of cGAS-cGAMP signaling in antiviral defense and immune adjuvant effects. Science. 2013;341(6152):1390–4. [CrossRef]

20 Manoury B, Hewitt EW, Morrice N, Dando PM, Barrett AJ, Watts C. An asparaginyl endopeptidase processes a microbial antigen for class II MHC presentation. Nature. 1998;396(6712):695–9. [CrossRef]

21 Manoury B, Mazzeo D, Fugger L, Viner N, Ponsford M, Streeter H, et al. Destructive processing by asparagine endopeptidase limits presentation of a dominant T cell epitope in MBP. Nat Immunol. 2002;3(2):169–74. [CrossRef]

22 Gough DJ, Messina NL, Clarke CJ, Johnstone RW, Levy DE. Constitutive type I interferon modulates homeostatic balance through tonic signaling. Immunity. 2012;36(2):166–74. [CrossRef]

23 Sun W, Lin Y, Chen L, Ma R, Cao J, Yao J, et al. Legumain suppresses OxLDL-induced macrophage apoptosis through enhancement of the autophagy pathway. Gene. 2018;652:16–24. [CrossRef]

24 Liu D, Zhang H, Huang YP, Gao YQ. Investigating the activation mechanism differences between human and mouse cGAS by molecular dynamics simulations. J Phys Chem B. 2023;127(22):5034–45. [CrossRef]